# Review of Form-Finding Methods for Tensegrity Structures

A.G. Tibert[*] and S. Pellegrino[†]

[*]Department of Structural Engineering, Royal Institute of Technology

SE-100 44 Stockholm, Sweden.

[†]Department of Engineering, University of Cambridge

Trumpington Street, Cambridge CB2 1PZ, U.K.

## Abstract

Seven form-finding methods for tensegrity structures are reviewed and classified. The three kinematical methods include an analytical approach, a non-linear optimisation, and a pseudo-dynamic iteration. The four statical methods include an analytical method, the formulation of linear equations of equilibrium in terms of force densities, an energy minimisation, and a search for the equilibrium configurations of the struts of the structure connected by cables whose lengths are to be determined, using a reduced set of equilibrium equations. It is concluded that the kinematical methods are best suited to obtaining only configuration details of structures that are already essentially known, the force density method is best suited to searching for new configurations, but affords no control over the lengths of the elements of the structure. The reduced coordinates method offers a greater control on elements lengths, but requires more extensive symbolic manipulations.

# Nomenclature

$a$      Side length of equilateral triangle

$\mathbf{A}$      $A_{ij} = \partial l_j / \partial q_i$

$\mathbf{C}$      Incidence matrix of free coordinates

$\mathbf{C}_f$      Incidence matrix of constrained coordinates

$\mathbf{C}_s$      Incidence matrix

$d$      Dimension of space

$\mathbf{d}$      Displacement vector

$\dot{\mathbf{d}}$      Velocity vector

$\ddot{\mathbf{d}}$      Acceleration vector

$\mathbf{D}$      Damping matrix

$\mathbf{D}$      Force density matrix

$E(\mathbf{p})$      Energy form associated to $\boldsymbol{\omega}$

$f$      External force

$\mathbf{f}$      External force vector

$g$      Generalised coordinate

$\mathbf{g}$      Vector of generalised coordinates

$H$      Height

$h$      Stage overlap

$\mathbf{K}$      Stiffness matrix

$l$      Length of element

$M$      Number of cables

$\mathbf{M}$      Mass matrix

$N$      Number of generalised coordinates

$\mathcal{N}$      Nullity of $\mathbf{D}$

$O$      Number of rigid elements

$\mathbf{p}_i$      Nodal coordinates, $[x_i,\ y_i,\ z_i]^{\mathrm{T}}$

$q$      Force density

$\mathbf{Q}$      $\mathrm{diag}(\mathbf{q})$

$R$      Radius

$t$      Force in element

$\mathbf{t}$      Vector of element forces

$v$      Number of polygon edges

$\mathbf{x}$      Vector of free $x$-coordinates

$\mathbf{x}_f$      Vector of constrained $x$-coordinates

| | |
|---|---|
| $\mathbf{x}_s$ | Vector of $x$-coordinates |
| $\alpha$ | Azimuth angle |
| $\delta$ | Declination angle |
| $\delta W$ | Virtual work |
| $\theta$ | Relative rotation |
| $\omega$ | Stress (equivalent to $q$) |
| $\boldsymbol{\omega}$ | Vector of stresses (equivalent to $\mathbf{q}$) |
| $\boldsymbol{\Omega}$ | Stress matrix (equivalent to $\mathbf{D}$) |

# 1 Introduction

New developments are currently taking place in the field of tensegrity structures, driven by a growing interest in "smart" structures whose shape can be actively adjusted and controlled. Because of the lack of physical connections between compression members, the joints of a tensegrity structure have a predictable, linear response over a wide range of different shapes, which can be very attractive, e.g. for deployable structures [1,2]. Also, earlier interest in tensegrity as a model for the structure of viruses [3] has recently extended to cellular [4] structures.

A key step in the design of tensegrity structures is the determination of their geometrical configuration, known as *form-finding*. Early studies by Fuller [5,6], Snelson [7] and Emmerich into the form of tensegrity structures used mainly regular, convex polyhedra as the basis for finding new configurations. This purely geometric research resulted in a large number of configurations which were later classified by Pugh [8] by identifying three pattern types: diamond, circuit and zig-zag. A large number of different tensegrities, with detailed schemes and advice on how to to build them can be found in Ref. [8].

However, physical models of these structures showed that the shape of the tensegrity corresponding to a particular polyhedron is different from that of the polyhedron. This happens, for example, both for the truncated tetrahedron, Fig. 1 and the expandable octahedron (icosahedron), Fig. 2. Hence, the self-stressed shape of a tensegrity is not identical to that of the polyhedron and, therefore, proper form-finding methods are needed to find the equilibrium configuration of even the simplest tensegrity structure [9].

Form-finding methods for tensegrity structures have been investigated by many authors, and recently by Connelly and Terrell [10], Vassart and Motro [11], and Sultan et al. [12]. Different approaches have been proposed by these authors, but the various methods have not been previously linked. We classify the existing methods into two broad families, kinematical and statical methods, and identify the advantages and limitations of each method. Closer scrutiny of the seemingly different approaches in Refs [10-12] reveals many links, indeed Vassart and Motro's force density method can be linked directly to the more abstract energy approach by Connelly.

This paper reviews the current state of the art in form-finding methods for tensegrity structures. Each method is explained and illustrated by means of examples. The technique recently developed by Vassart and Motro is found to be particularly suitable to find new tensegrity structures that meet a set of given, although general requirements. Several examples are shown of

how to do this in practice.

The paper is laid out as follows. Section 2 introduces three *kinematical methods*, which determine the geometry of a given tensegrity structure by maximising the lengths of the struts while keeping constant the given lengths of the cables. The three methods consist in (i) an analytical approach, (ii) a non-linear optimisation method, and (iii) a pseudo-dynamic iterative method. Section 3 introduces four *statical methods*, which determine the possible equilibrium configurations of a tensegrity structure with given topology, i.e. a given number of nodes and connecting elements between them. Methods (i) and (ii) establish linear nodal equations of equilibrium in terms of so-called force densities and solve these equations for the nodal coordinates, either analytically in method (i) or by setting up a force density matrix in mehtod (ii). Method (iii) is based on an energy minimisation approach, which is shown to produce a matrix identical to the force-density matrix, and introduces the concept of super-stable tensegrities. Method (iv) searches for equilibrium configurations of a set of rigid bodies, i.e. the struts of the tensegrity structure, connected by cables whose lengths are to be determined. A reduced set of equilibrium equations for the struts are determined by virtual work, making use of symmetry conditions, and are then solved in symbolic form. Section 4 shows examples of form-finding analyses done by means of the second static method. Section 5 compares the methods presented and concludes the paper.

# 2 Kinematical Methods

The characteristic of these methods is that the lengths of the cables are kept constant while the strut lengths are increased until a *maximum* is reached. Alternatively, the strut lengths may be kept constant while the cable lengths are decreased until they reach a *minimum*. This approach mimics the way in which tensegrity structures are built in practice, without explicitly requiring that the cables be put in a state of pre-tension.

## 2.1 Analytical Solutions

Consider a simple structure consisting of cables arranged along the edges of a regular prism, plus a number of struts connecting the $v$ vertices of the bottom polygon to corresponding vertices of the upper polygon. Depending on the value of $v$ and the offset between vertices connected by a strut, there is a special rotation angle $\theta$ between the top and bottom polygons for which a

5

tensegrity structure is obtained.

A compact description of the geometry of this problem, taking advantage of its symmetry, was introduced by Connelly and Terrell [10], as follows. Figure 3 shows the elements connected to one of the nodes of the bottom polygon. In the starting configuration the lateral cable, 1 2, is vertical and the angle between the ends of the strut is $2\pi j/v$ where $j$ is an integer smaller than $v$.

The coordinates of nodes 1–5 are:

$$
\begin{aligned}
\mathbf{p}_1 &= [R,\ 0,\ 0], \\
\mathbf{p}_2 &= [R\cos\theta,\ R\sin\theta,\ H], \\
\mathbf{p}_3 &= \left[R\cos\left(\theta + \frac{2\pi j}{v}\right),\ R\sin\left(\theta + \frac{2\pi j}{v}\right),\ H\right], \\
\mathbf{p}_4 &= \left[R\cos\left(\frac{2\pi}{v}\right),\ -R\sin\left(\frac{2\pi}{v}\right),\ 0\right], \\
\mathbf{p}_5 &= \left[R\cos\left(\frac{2\pi}{v}\right),\ R\sin\left(\frac{2\pi}{v}\right),\ 0\right].
\end{aligned}
$$

The kinematic form-finding proceeds as follows, by considering the square of the lengths of the lateral cable, 1 2, and strut, 1 3,

$$
l_c^2 = 2R^2(1 - \cos\theta) + H^2, \tag{1}
$$

$$
l_s^2 = 2R^2\left[1 - \cos\left(\theta + \frac{2\pi j}{v}\right)\right] + H^2, \tag{2}
$$

where the subscripts $c$ and $s$ denote cable and strut, respectively.

Equation (2) can be rewritten as:

$$
l_s^2 = 4R^2 \sin\left(\theta + \frac{\pi j}{v}\right)\sin\frac{\pi j}{v} + l_c^2. \tag{3}
$$

For a given cable length $l_c$ the length of the strut $l_s$ is maximised for

$$
\theta = \pi\left(\frac{1}{2} - \frac{j}{v}\right) \tag{4}
$$

The simplicity of the kinematical method for structures with $v$-fold symmetry is mirrored by the static method, see Section 3.1, but for other, non-symmetric, cases the present formulation becomes infeasible due to the large number of variables required to describe a general configuration.

6

## 2.2 Non-Linear Programming

This general method, proposed by Pellegrino [13], turns the form-finding of any tensegrity structure into a constrained minimisation problem. Starting from a system for which the element connectivity and nodal coordinates are known, one or more struts are elongated, maintaining fixed length ratios, until a configuration is reached in which their length is maximised. The general constrained minimisation problem has the form:

$$\text{Minimise} \quad f(x, y, z)$$
$$\text{subject to} \quad g_i(x, y, z) = 0 \quad \text{for } i = 1, \dots, n \tag{5}$$

where the objective function $f(x, y, z)$ is, for example, the negative length of one of the struts. Pellegrino [13] applied this method to two tensegrities: the triangular prism and the truncated tetrahedron.

The triangular tensegrity prism, Fig. 10, has nine cables of length $l_c = 1$ and three struts. One of the base triangles is fixed, hence three of its six nodes are fixed in space. The constrained minimisation problem has the form:

$$\text{Minimise} \quad -l_{s1}^2$$

$$\text{subject to} \begin{cases} l_{c1}^2 - 1 = 0 \\ l_{c2}^2 - 1 = 0 \\ \qquad \vdots \\ l_{c6}^2 - 1 = 0 \\ l_{s2}^2 - l_{s1}^2 = 0 \\ l_{s3}^2 - l_{s1}^2 = 0 \end{cases} \tag{6}$$

where $c1, c2, ..., c6$ denote the six remaining cables and $s1, s2$ and $s3$ the struts. This problem can be solved, for example, using the constrained optimisation routine `fmincon` in Matlab [14]. The final length of the struts is 1.468, compared to the theoretical value of $\sqrt{1 + 2/\sqrt{3}} \approx 1.4679$ obtained from Eqns. (3)–(4).

Similarly, in the case of the truncated tetrahedron, Fig. 1, there are six struts and 18 cables. The objective function to be minimised, equal to the negative length of one of the struts, has to satisfy 20 constraint equations, 15 on the cable lengths plus 5 on the struts. The final length of the struts is 2.2507. Note that the strut length obtained from a purely geometric analysis of the truncated tetrahedron is $\sqrt{5} \approx 2.236$, hence the slight warping of the hexagonal faces leads to an increase of the strut lengths by 0.7%.

An advantage of the non-linear programming approach is that it makes use of general purpose, standard software. However, the number of constraint equations increases with the number of elements and so this approach is not feasible for larger systems. Also, although different geometric configurations of structures with the same topology can be found by specifying different relationships between the lengths of the struts, there is no direct way of controlling the corresponding variation in the state of prestress.

## 2.3   Dynamic Relaxation

The method of dynamic relaxation, that had already been successfully used for membrane and cable net structures [15,16], was put forward by Motro [17] and Belkacem [18] as a general form-finding method for tensegrity structures.

For a structure in a given initial configuration and subject to given external forces the equilibrium of configuration can be computed by integrating the following fictitious dynamic equations

$$\mathbf{M\ddot{d}} + \mathbf{D\dot{d}} + \mathbf{Kd} = \mathbf{f} \tag{7}$$

where $\mathbf{K}$ is a stiffness matrix, $\mathbf{M}$ a mass matrix, $\mathbf{D}$ a damping matrix, $\mathbf{f}$ the vector of external forces, and $\mathbf{\ddot{d}}$, $\mathbf{\dot{d}}$ and $\mathbf{d}$ the vectors of acceleration, velocity and displacement from the initial configuration, respectively. Both $\mathbf{M}$ and $\mathbf{D}$ are taken to be diagonal, for simplicity, and the velocities and displacements are initially set to zero.

There are several ways of carrying out a form-finding analysis, for example by prescribing for each element of the structure a constitutive relationship of the type

$$t = t_0 + ke \tag{8}$$

where $t$ is the axial force and $e$ the extension —measured from the initial configuration— of the element; $t_0$ is the desired prestress and $k$ a fictitious, small axial stiffness. In any current configuration of the structure, nodal equations of equilibrium are used to compute out-of-balance forces from which the current acceleration can be obtained through Eq. (7). The resulting system of uncoupled equilibrium equations can then be integrated using a centred finite difference scheme.

The coefficients of the damping matrix are usually given all the same value, chosen such as to maximise the speed of convergence to the equilibrium configuration. Alternatively, a technique called *kinetic damping* can be used, whereby the undamped motion of the structure is traced.

When a local peak in the total kinetic energy of the structure is detected, all velocity components are set to zero. The process is then repeated, starting from the current configuration, until the peak kinetic energy becomes sufficiently small [16].

Motro [17] applied the dynamic relaxation method to the form-finding of the triangular tensegrity prism. The lengths of the cables were held constant while the struts were gradually elongated, until a state of pre-stress was set up in the structure. This analysis converged to $l_s/l_c = 1.468$.

Belkacem [18] analysed the triangular and square tensegrity prisms, and also the expandable octahedron. The results for the tensegrity prisms were compared with the theoretical values obtained from Eq. (3) and those for the expandable octahedron to the results of a statical method. The relative errors in the nodal coordinates were 0.2%, 4%, and 2% respectively. For the tensegrity prisms errors in the rotation angle $\theta$ of 1% and 8%, respectively, were obtained. An analysis of the truncated tetrahedron [19] gave a ratio $l_s/l_c$ slightly greater than 2.24 and close to the value determined by Pellegrino [13].

Motro et al. [20] later concluded that the dynamic relaxation method has good convergence properties for structures with only a few nodes but is not effective when the number of nodes increases. Also, the method becomes rather cumbersome if several different ratios between strut lengths and cable lengths are desired, which restricts its applicability to less regular structural forms. However, the same restriction applies to kinematical methods in general.

## 3 Statical Methods

The general characteristic of these methods is that a relationship is set up between equilibrium configurations of a structure with given topology and the forces in its members. This relationship is then analysed by various methods.

### 3.1 Analytical Solutions

Kenner [21] used node equilibrium and symmetry arguments to find the configuration of the expandable octahedron, Fig. 2, whose six identical struts are divided into three pairs and the distance between the struts in each pair is exactly half the strut length. Other, more complex, spherical tensegrities with polyhedral geometries, i.e. the cuboctahedron and the icosidodecahe-

dron, were also analysed using the same approach.

Recently, Connelly and Terrell [10] have used an equilibrium approach to find the prestress stable form of rotationally symmetric tensegrities. To set up a system of linear equilibrium equations, they used force density,[1] i.e. force divided by length, as variable for each element.

Denoting by $q_{ij}$ the force density in element $ij$ —note that $q_{1,4} = q_{1,5}$ due to symmetry— the equilibrium of node 1 in the $z$- and $y$-direction can be written as

$$q_{1,2}H + q_{1,3}H = 0 \tag{9}$$

and

$$q_{1,2}R\sin\theta + q_{1,3}R\sin\left(\theta + \frac{2\pi j}{v}\right) = 0, \tag{10}$$

respectively. Equations (9) and (10) give

$$q_{1,2}\left[\sin\theta - \sin\left(\theta + \frac{2\pi j}{v}\right)\right] = 0. \tag{11}$$

The only solution of Eq. (11) for which all of the cables are in tension is [10]

$$\theta = \pi\left(\frac{1}{2} - \frac{j}{v}\right). \tag{12}$$

The values of $\theta$ for tensegrity modules with $v$ going from 3 to 6 are given in Table 1. Note that Eq. (12) is identical to Eq. (4), as expected.

## 3.2   Force Density Method

The force density method for cable structures, first proposed by Linkwitz and Schek in 1971 [22,23], uses a simple mathematical trick to transform the non-linear equilibrium equations of the nodes into a set of linear equations. For example, the equilibrium equation in the $x$-direction for node $i$ is

$$\sum_j \frac{t_{ij}}{l_{ij}}(x_i - x_j) = f_{ix} \tag{13}$$

Although this may appear to be a linear equation in the nodal coordinates, it is actually non-linear because the lengths $l_{ij}$ in the denominator are also functions of the coordinates. These equations can be linearised by introducing for each element the force density

$$q_{ij} = t_{ij}/l_{ij} \tag{14}$$

---

[1]Also called tension coefficient, see Ref. [24].

whose value needs to be known at the start of the form-finding process.

For a structure with $b$ elements and $n$ nodes the equilibrium equations in the $x$-direction can be written as

$$\mathbf{C}_s^{\mathrm{T}}\mathbf{Q}\mathbf{C}_s\mathbf{x}_s = \mathbf{f}_x, \tag{15}$$

where $\mathbf{C}_s$ is the incidence matrix, see below, $\mathbf{Q}$ a diagonal matrix containing the force densities, $\mathbf{x}_s$ a column vector of $x$-coordinates, and $\mathbf{f}_x$ a column vector of external nodal forces in the $x$-direction. Equations identical to (15) can be written also in term of the $y$- and $z$ coordinates.

The incidence matrix $\mathbf{C}_s$, of size $b \times n$, describes the connectivity of the structure; if an element connects nodes $i$ and $j$, then the corresponding row of $\mathbf{C}_s$ has $+1$ in column $i$ and $-1$ in column $j$. If the coordinates of some of the nodes are given, e.g. these nodes are attached to a foundation, $\mathbf{C}_s$ can be partitioned as

$$\mathbf{C}_s = \begin{bmatrix} \mathbf{C} & \mathbf{C}_f \end{bmatrix}, \tag{16}$$

where the restrained nodes have been put at the end of the numbering sequence. Equation (15) can now be written as

$$\mathbf{C}^{\mathrm{T}}\mathbf{Q}\mathbf{C}\mathbf{x} = \mathbf{f}_x - \mathbf{C}^{\mathrm{T}}\mathbf{Q}\mathbf{C}_f\mathbf{x}_f, \tag{17}$$

where $\mathbf{x}$ and $\mathbf{x}_f$ are the column vectors of unknown and given $x$-coordinates, respectively. Equation (17), together with analogous equations for the $y$- and $z$-directions, can be solved to find the nodal coordinates. Usually, the external loads are zero during form-finding.

In a structure consisting of cables only all tension coefficients are positive, i.e. $q_{ij} > 0$, and hence $\mathbf{C}^{\mathrm{T}}\mathbf{Q}\mathbf{C}$ is positive definite and, thus, invertible. Therefore, there is always a unique solution to the form-finding problem. The same approach can be extended to the form-finding of membrane structures by converting the stresses in the membrane into forces in a virtual cable net [25,26].

A similar formulation can be applied to the form-finding of tensegrity structures, but as these structures are self-stressed, usually there are no foundation nodes as well as no external loads. Hence, Eq. (15) becomes

$$\mathbf{D}\mathbf{x}_s = \mathbf{0}, \tag{18}$$

where $\mathbf{D} = \mathbf{C}_s^{\mathrm{T}}\mathbf{Q}\mathbf{C}_s$ and analogous equations hold in the $y$- and $z$-directions.

The force density matrix $\mathbf{D}$ can be written directly [11], without going through $\mathbf{C}_s$ and $\mathbf{Q}$, following the scheme

$$
D_{ij} = \begin{cases} -q_{ij} & \text{if } i \neq j, \\ \sum_{k \neq i} q_{ik} & \text{if } i = j, \\ 0 & \text{if } i \text{ and } j \text{ are not connected.} \end{cases} \tag{19}
$$

Note that the matrix $\mathbf{D}$ is always square and singular, with a nullity of at least 1 since the row and column sums are zero, by Eq. (19). Unlike the matrix $\mathbf{C}^{\mathrm{T}} \mathbf{Q} \mathbf{C}$ for a cable net attached to foundation nodes, which is positive definite see page 120 of Ref. [22], the $\mathbf{D}$ matrix for a tensegrity is semi-definite and, due to the presence of compression elements, with $q_{ij} < 0$, several complications can arise during form-finding. A practical procedure for finding a set of force densities that yield a matrix $\mathbf{D}$ with the required rank was given by Vassart [27]. Further details will be given in Section 4.

## 3.3   Energy Method

In the following, some key main findings of Connelly [28] will be summarised using as far as possible the original terminology.

A configuration of $n$ ordered points in $d$-dimensional space is denoted by

$$
\mathbf{p} = [\mathbf{p}_1, \ \mathbf{p}_2, \ ..., \ \mathbf{p}_n]^{\mathrm{T}}. \tag{20}
$$

A *tensegrity framework* $G(\mathbf{p})$ is the graph on $\mathbf{p}$ where each edge is designated as either a cable, a strut or a bar; cables cannot increase in length, struts cannot decrease in length and bars cannot change length. A stress state $\boldsymbol{\omega}$ for $G(\mathbf{p})$ is a self-stress if the following condition holds at each node $i$:

$$
\sum_j \omega_{ij} \left( \mathbf{p}_j - \mathbf{p}_i \right) = \mathbf{0}, \tag{21}
$$

where $\omega_{ij} \geq 0$ for cables, $\omega_{ij} \leq 0$ for struts, and no condition is stipulated for the bars. Comparing Eq. (21) with the equilibrium equations for the same node written in terms of force densities, it is obvious that the stresses $\omega_{ij}$ are identical to the force densities $q_{ij}$.

Satisfying the above equilibrium condition is a necessary but not sufficient condition for the tensegrity framework to be in a stable equilibrium configuration. A basic principle in the analysis of the stability of structures is that the total potential energy functional should be at a local

minimum for a given configuration to be stable. In analogy with the total potential energy, ref. [29] defines the following energy form associated with the stress $\boldsymbol{\omega}$:

$$E(\mathbf{p}) = \frac{1}{2} \sum_{ij} \omega_{ij} \|\mathbf{p}_j - \mathbf{p}_i\|^2. \tag{22}$$

The idea is that when the end points of an element are displaced, energy builds up as a function of the square of the extension. The function in Eq. (22) is set up to have an absolute minimum corresponding to the rest length of the element [28]. All members are assumed to behave as linear elastic springs. The cables, which take only tension, have a rest length of zero while the struts, which take only compression, have an infinite rest length.

Let

$$\overline{\mathbf{p}} = \begin{bmatrix} \mathbf{x} \\ \mathbf{y} \\ \mathbf{z} \end{bmatrix} \tag{23}$$

be a column vector, of length $dn$, containing the $x$-coordinates of $\mathbf{p}$, followed by the $y$-coordinates, etc. Then, Eq. (22) can be written as the quadratic form:

$$E(\mathbf{p}) = \frac{1}{2} \overline{\mathbf{p}}^{\mathrm{T}} \begin{bmatrix} \boldsymbol{\Omega} & & \\ & \ddots & \\ & & \boldsymbol{\Omega} \end{bmatrix} \overline{\mathbf{p}}, \tag{24}$$

where the elements of $\boldsymbol{\Omega}$ are given by

$$\Omega_{ij} = \begin{cases} -\omega_{ij} & \text{if } i \neq j, \\ \sum_{k \neq i} \omega_{ik} & \text{if } i = j, \\ 0 & \text{if there is no connection between } i \text{ and } j. \end{cases} \tag{25}$$

Note that $\boldsymbol{\Omega}$ is identical to $\mathbf{D}$, hence the above formulation provides a deeper insight into the characteristics of the force density method and how it can be used to find stable equilibrium configurations of tensegrity structures. The link between the force density method and energy minimisation was first pointed out in Section 2 of Ref. [30] and later in Section 4 of Ref. [22].

A necessary condition for the tensegrity framework to be prestress stable in the configuration $\mathbf{p}$ is that the quadratic form $E(\mathbf{p})$ has a local minimum at $\mathbf{p}$. The positive definiteness of $E(\mathbf{p})$ is directly related to that of $\boldsymbol{\Omega}$ but expecting positive definiteness is unrealistic, because —as already noted above for $\mathbf{D}$— the nullspace of $\boldsymbol{\Omega}$ contains at least the non-trivial vector $[1, ..., 1]^{\mathrm{T}}$.

The strongest type of prestress stability, named *super stability* by Connelly [31], requires prestress stability with the additional condition that $\mathbf{\Omega}$ is positive semi-definite with maximal rank. The maximal rank of $\mathbf{\Omega}$ for a structure in $d$-dimensional space that does not in fact lie in a subspace of smaller dimension, see the examples in Section 4.1, is $n - d - 1$. Hence, to design a super stable tensegrity framework one has to find a set of force densities such that the nullity $\mathcal{N}$ of $\mathbf{\Omega}$ is $d + 1$.

For example, consider the two-dimensional ($d = 2$) tensegrity structure in Fig. 4 where the outside edges are cables and the diagonals are struts. A stress equal to 1 in the cables and $-1$ in the struts is a self-stress for this structure. The stress, i.e. force density, matrix is [29]:

$$\mathbf{\Omega} = \begin{bmatrix} 1 & -1 & 1 & -1 \\ -1 & 1 & -1 & 1 \\ 1 & -1 & 1 & -1 \\ -1 & 1 & -1 & 1 \end{bmatrix}, \tag{26}$$

which is positive semi-definite with nullity 3. Hence, the tensegrity structure in Fig. 4 is super stable [31].

Connelly and Back [32] have analysed tensegrity structures with different types of symmetry using this method. Their initial assumption was that there is a symmetric state of self-stress with a force density of 1 in each cable and $-\omega_s$ in each strut. A further assumption was that there are two types of cables but only one type of strut, arranged such that satisfying equilibrium at only one node of the structure implies, by symmetry, that it is satisfied also at all other nodes. The force density in the strut is chosen such that the structure is super stable [31,32].

A complete catalogue of all the tensegrity structures that are possible for each symmetry group has been produced, using group theory. Although some of the systems in the catalogue have struts that go through each other, and therefore are of limited practical interest, the catalogue contains many solutions that were previously unknown.

## 3.4   Reduced Coordinates

This method was introduced by Sultan et al. [12]. Consider a tensegrity structure whose $b$ elements consist of $M$ cables and $O$ struts. The struts are considered as a set of bilateral constraints acting on the cable structure. Hence, a set of independent, generalised coordinates

$\mathbf{g} = [g_1, \ g_2, \dots, \ g_N]^{\mathrm{T}}$ is defined, which define the position and orientation of these struts.[2]

Consider a state of self-stress for the structure and let $t_j$ be the axial force in a generic cable element $j$; the cable forces $\mathbf{t} = [t_1, \ t_2, \dots, t_M]^{\mathrm{T}}$ are in equilibrium with appropriate forces in the struts and zero external loads. A set of equilibrium equations relating the forces in the cables, but without showing explicitly the forces in the struts, can be obtained from virtual work.

Consider a virtual displacement $\delta\mathbf{g}$ of the structure that involves no extension of the struts. The change of length of cable $j$ is

$$\delta l_j = \sum_{i=1}^{N} \frac{\partial l_j}{\partial g_i} \delta g_i. \tag{27}$$

Considering all cables, Eq. (27) gives

$$\delta\mathbf{l} = \mathbf{A}^{\mathrm{T}}\delta\mathbf{g}, \tag{28}$$

where the elements of the $N \times M$ matrix $\mathbf{A}$ are

$$A_{ij} = \frac{\partial l_j}{\partial g_i}. \tag{29}$$

Because the extensions of the struts are zero, the virtual work in the struts is also zero and so the total internal work, from the cables only, is

$$\mathbf{t}^{\mathrm{T}}\delta\mathbf{l} = (\mathbf{At})^{\mathrm{T}}\delta\mathbf{g} \tag{30}$$

For the structure to be in equilibrium, this must be zero for any virtual displacement $\delta\mathbf{g}$. This gives the following reduced equilibrium equations

$$\mathbf{At} = \mathbf{0}. \tag{31}$$

For this equation to have a nontrivial solution it is required that

$$\mathrm{rank}\mathbf{A} < M \tag{32}$$

where only solutions that are entirely positive are of interest, i.e.

$$t_j > 0 \ \ \text{for } j = 1, 2, \dots, M \tag{33}$$

General analytical conditions that govern the form of a tensegrity structure of given topology can be obtained by analysing Eqs (32) and (33).

---

[2]If $d = 2$ three generalised coordinates are required for each strut, hence $N = 3 \times O$; if $d = 3$ then $N = 5 \times O$.

Sultan [33] applied this method to a tensegrity tower of which Fig. 6 shows a simple, two-stage example. The same structure had been previously considered by Snelson [7], see Fig. 7. The tower consists of three struts per stage, held in place by three sets of cables —saddle, vertical, and diagonal— between two rigid triangular plates at the top and bottom; in Fig. 6 note the definition of the overlap $h$. Having shown that a structure in which the rigid plates have been replaced by cables has the same equilibrium configuration as the original structure, but involves a smaller number of unknown cable forces, Sultan analysed this simpler problem.

The first step in the form-finding process is to identify a set of generalised coordinates which describe the configuration of this structure. The 18 coordinates chosen by Sultan [33] for the two stage tower were

- for each strut, the azimuth angle $\alpha_j$, i.e. the angle between the vertical plane containing the strut and the $x$-$z$ plane, and the colatitude $\delta_j$, i.e. the angle between the strut and the $z$-axis, and

- three translation and three rotation parameters defining the position and orientation of the rigid plate at the top with respect to the bottom one.

By using symbolic manipulation software, e.g. Maple or Mathematica, the length of each cable can be expressed in terms of the 18 coordinates and then differentiated to obtain the $18 \times 18$ matrix $\mathbf{A}$, in symbolic form. At this stage, the final shape of the structure is still unknown and the existence of a prestressable configuration is dependent on finding a suitable set of strut lengths. Sultan [33] reduced the number of independent generalised coordinates by considering only symmetric configurations, with the same azimuth, $\alpha$, and colatitude, $\delta$, and by considering a fixed position of the top plate. Then, by assuming a special symmetry in $\mathbf{t}$, the problem could be reduced even further, to $3 \times 3$ with the forces in the diagonal, saddle and vertical cables remaining as the only unknowns. Finally, applying to this reduced matrix the condition for the existence of non-trivial solutions, rank $\mathbf{A} = 2$ equivalent to

$$\det \mathbf{A} = 0 \tag{34}$$

gave a quadratic equation that could be solved for the overlap $h$

$$h = \begin{cases} \dfrac{1}{2\tan\delta\cos\left(\alpha+\dfrac{\pi}{6}\right)}\left(\sqrt{\dfrac{a^2}{3}-3l^2\sin^2\delta\cos^2\left(\alpha+\dfrac{\pi}{6}\right)}\right. \\ \left. -\dfrac{a}{\sqrt{3}}+l\sin\delta\cos\left(\alpha+\dfrac{\pi}{6}\right)\right) & \text{if } \alpha\neq\dfrac{\pi}{3}, \\ \dfrac{l\cos\delta}{2} & \text{if } \alpha=\dfrac{\pi}{3}. \end{cases} \tag{35}$$

Here, $a$ is the side length of the equilateral triangles at the top and bottom of the tower, and $l$ the length of the strut.

A particular, symmetric configuration in which all the nodes lie on the surface of a cylinder is defined by the following relation between $\delta$ and $\alpha$:

$$\delta = \arcsin\left[\frac{2a}{l\sqrt{3}}\sin\left(\alpha+\frac{\pi}{3}\right)\right] \tag{36}$$

For towers with more than two stages $\mathbf{A}$ was still derived using symbolic software, but Eq. (34) was then solved numerically. Sultan [33] successfully applied this form-finding method to towers with up to nine stages.

# 4   Implementation of Force Density Method

The force density method has been outlined in Section 3.2. This section will deal with procedures to actually find super-stable tensegrities, i.e. with positive definite matrix $\mathbf{D}$ with nullity $\mathcal{N} = d+1$. Vassart and Motro [11] have listed three techniques for finding a set of force densities that achieve the required nullity: (i) intuitive; (ii) iterative; and (iii) analytical.

Of these three techniques, the first is suitable for systems with only a few members, and will be illustrated in Section 4.1; the second technique is based on a trial-and-error, or more refined search for a set of force densities that yield the required nullity. The third technique is the most effective; $\mathbf{D}$ is analysed in symbolic or semi-symbolic form, in the case of systems with a large number of elements [11]. The following examples show how this is done in practice, for structures of increasing complexity.

## 4.1   A Two-Dimensional Example

Consider the hexagonal tensegrity shown in Fig. 8. For it to be super stable, the nullity of $\mathbf{D}$ has to be three, but it is interesting to consider also the cases $\mathcal{N} = 1, 2$ to better understand why

in Section 3.3 it was stated that one must look for sets of force densities that make rank $\mathbf{D} = n - d - 1$.

*Case $\mathcal{N} = 1$*

Most sets of force densities yield a $\mathbf{D}$ matrix with nullity one. For example, the *general* set $\mathbf{q}_1 = [1, 2, 3, 4, 5, 6, -7, -8, -9]^\mathrm{T}$ gives

$$\mathbf{D}_1 = \begin{bmatrix} 0 & -1 & 0 & 7 & 0 & -6 \\ -1 & -5 & -2 & 0 & 8 & 0 \\ 0 & -2 & -4 & -3 & 0 & 9 \\ 7 & 0 & -3 & 0 & -4 & 0 \\ 0 & 8 & 0 & -4 & 1 & -5 \\ -6 & 0 & 9 & 0 & -5 & 2 \end{bmatrix} \tag{37}$$

The nullspace of $\mathbf{D}_1$ is spanned by $[1, 1, 1, 1, 1, 1]^\mathrm{T}$ —see Ref. [34] for further details on how to compute a basis for a nullspace— which, through Eq. (18) and the analogous equation in the $y$-coordinates, gives the configuration $\mathbf{x} = [x_1, \dots, x_6]^\mathrm{T} = [\alpha, \alpha, \alpha, \alpha, \alpha, \alpha]^\mathrm{T}$ and $\mathbf{y} = [y_1, \dots, y_6]^\mathrm{T} = [\beta, \beta, \beta, \beta, \beta, \beta]^\mathrm{T}$. Here, $\alpha$ and $\beta$ can take arbitrary values. Of course, this solution corresponds to configurations of the structure where all nodes coincide and so the whole structure is reduced to a single point, which is of little practical interest.

*Case $\mathcal{N} = 2$*

Next, we choose uniform force densities in all cable elements and in *two* of the struts force densities of half those in the cables; the force density in the third cable is arbitrary. For example, for $\mathbf{q}_2 = [2, 2, 2, 2, 2, 2, -1, -1, -3]^\mathrm{T}$ we obtain

$$\mathbf{D}_2 = \begin{bmatrix} 3 & -2 & 0 & 1 & 0 & -2 \\ -2 & 3 & -2 & 0 & 1 & 0 \\ 0 & -2 & 1 & -2 & 0 & 3 \\ 1 & 0 & -2 & 3 & -2 & 0 \\ 0 & 1 & 0 & -2 & 3 & -2 \\ -2 & 0 & 3 & 0 & -2 & 1 \end{bmatrix} \tag{38}$$

It can be readily verified that columns five and six are *dependent*, and hence that the nullspace of $\mathbf{D}_2$ is spanned by $[-1, -1, 0, 1, 1, 0]^\mathrm{T}$ and $[2, 2, 1, 0, 0, 1]^\mathrm{T}$. Hence, denoting by $\alpha, \beta$ the $x$-coordinates of nodes 5, 6 respectively, and by $\gamma, \delta$ their $y$-coordinates, the configuration of the system is described by $\mathbf{x} = [-\alpha + 2\beta, -\alpha + 2\beta, \beta, \alpha, \alpha, \beta]^\mathrm{T}$ and $\mathbf{y} = [-\gamma + 2\delta, -\gamma + 2\delta, \delta, \gamma, \gamma, \delta]^\mathrm{T}$.

This configuration corresponds to all nodes lying on a straight line, as shown in Fig. 9(a), and is again of little practical interest.

*Case $\mathcal{N} = 3$*

Finally, we choose *uniform force densities* both in the cable elements and in the struts, in a ratio of two to one. For example, $\mathbf{q}_3 = [2, 2, 2, 2, 2, 2, -1, -1, -1]^{\mathrm{T}}$ gives

$$
\mathbf{D}_3 = \begin{bmatrix}
3 & -2 & 0 & 1 & 0 & -2 \\
-2 & 3 & -2 & 0 & 1 & 0 \\
0 & -2 & 3 & -2 & 0 & 1 \\
1 & 0 & -2 & 3 & -2 & 0 \\
0 & 1 & 0 & -2 & 3 & -2 \\
-2 & 0 & 1 & 0 & -2 & 3
\end{bmatrix}
\tag{39}
$$

Here, columns four, five and six are dependent, hence the nullspace of $\mathbf{D}_3$ is spanned by $[1, 2, 2, 1, 0, 0]^{\mathrm{T}}$, $[-2, -3, -2, 0, 1, 0]^{\mathrm{T}}$, and $[2, 2, 1, 0, 0, 1]^{\mathrm{T}}$. Denoting by $\alpha, \beta, \gamma$ the free $x$-coordinates of nodes 4,5,6, respectively, and $\delta, \epsilon, \zeta$ their $y$-coordinates, the system configuration is given by $\mathbf{x} = [\alpha - 2\beta + 2\gamma, 2\alpha - 3\beta + 2\gamma, 2\alpha - 2\beta + \gamma, \alpha, \beta, \gamma]^{\mathrm{T}}$ and $\mathbf{y} = [\delta - 2\epsilon + 2\zeta, 2\delta - 3\epsilon + 2\zeta, 2\delta - 2\epsilon + \zeta, \delta, \epsilon, \zeta]^{\mathrm{T}}$.

The original solution in Fig. 8 is re-obtained for $\alpha = -1$, $\beta = -1/2$, $\gamma = 1/2$, $\delta = 0$, $\epsilon = -\sqrt{3}/2$, $\zeta = -\sqrt{3}/2$. However, note that, despite the force densities $\mathbf{q}_3$ being symmetric, this solution gives the configuration shown in Fig. 9(b), which has only two-fold symmetry, for e.g. $\alpha = -1$, $\beta = -1/2$, $\gamma = 1$, $\delta = 0$, $\epsilon = -\sqrt{3}/2$, $\zeta = -1/2$. The reason why it is possible to find less symmetric or even asymmetric configurations for a given, symmetric state of force densities is because the element lengths are not explicitly set in the force density formulation.

In concluding, it is noted that the particular $\mathbf{q}_3$ considered above was obtained after noticing that in the configuration shown in Fig. 8 the force densities must have a particular distribution, to satisfy nodal equilibrium. However, by carrying out a symbolic analysis of the force density matrix other solutions were subsequently found. For example, an alternative choice is $\mathbf{q}_4 = [1, 2, 1, 2, 1, 2, -2/3, -2/3, -2/3]^{\mathrm{T}}$, for which a particular configuration (with $\alpha, \beta$, etc. as in the original solution) is that shown in Fig. 9(c).

## 4.2  Tensegrity Prisms

Consider the structure shown in Fig. 10.  A set of force densities with 3-fold symmetry is prescribed as follows. The force densities in the cables forming the bottom and top triangles are $q_b$ and $q_t$, respectively; they are $q_l$ in the lateral cables and $q_s$ in the struts. Assuming that the top and bottom triangles lie in horizontal planes, vertical equilibrium gives $q_s = -q_l$, cf. Eq. (9).

Hence, the $\mathbf{D}$ matrix can be set up in terms of only three force densities

$$\mathbf{D} = \begin{bmatrix} 2q_t & -q_t & -q_t & -q_l & 0 & q_l \\ -q_t & 2q_t & -q_t & q_l & -q_l & 0 \\ -q_t & -q_t & 2q_t & 0 & q_l & -q_l \\ -q_l & q_l & 0 & 2q_b & -q_b & -q_b \\ 0 & -q_l & q_l & -q_b & 2q_b & -q_b \\ q_l & 0 & -q_l & -q_b & -q_b & 2q_b \end{bmatrix} \tag{40}$$

By Gaussian elimination $\mathbf{D}$ is reduced to the upper echelon form [34]

$$\mathbf{U} = \begin{bmatrix} q_l & 0 & -q_l & -q_b & -q_b & 2q_b \\ 0 & q_l & -q_l & q_b & -2q_b & q_b \\ 0 & 0 & 0 & -q^* & 0 & q^* \\ 0 & 0 & 0 & 0 & q^* & -q^* \\ 0 & 0 & 0 & 0 & 0 & 0 \\ 0 & 0 & 0 & 0 & 0 & 0 \end{bmatrix} \tag{41}$$

where $q^* = (q_l^2 - 3q_b q_t)/q_l$. Since $q_l \neq 0$, rank $\mathbf{D}$ is either four, if $q^* \neq 0$, or two, if $q^* = 0$. If super stability is required, then we need $\mathcal{N} = 4$, i.e. rank $\mathbf{D} = 2$ and so $q^* = 0$.

Any set of positive cable force densities that satisfies the condition

$$q_l^2 - 3q_b q_t = 0 \tag{42}$$

will do but Vassart [27] presents two interesting cases: (i) $q_t = q_b$ and (ii) $q_t = q_l$. In both cases, the last four coordinates are "free"; denoting the free $x$-coordinates, for example, by $\alpha, \beta, \gamma, \delta$, in case (i) the configuration of the structure is described by $\mathbf{x} = [\alpha + (\beta + \gamma - 2\delta)/\sqrt{3}, \alpha + (-\beta + 2\gamma - \delta)/\sqrt{3}, \alpha, \beta, \gamma, \delta]$, similarly for $y$ and $z$. In case (ii) the configuration of the structure is described by $\mathbf{x} = [\alpha + (\beta + \gamma - 2\delta)/3, \alpha + (-\beta + 2\gamma - \delta)/3, \alpha, \beta, \gamma, \delta]$. The rotationally symmetric configurations, obtained by giving appropriate values to $\alpha$, etc. are shown in Fig. 11.

Obviously, changing the relation between $q_t$ and $q_b$ while keeping $q_l$ fixed, changes the relative sizes of the top and bottom triangles. Again, many geometrically non-symmetric configurations may be found by appropriate choices of the coordinates of the free nodes.

## 4.3   More Complex Systems

The earlier part of this section has shown applications of the force density method to the form-finding of some relatively straightforward tensegrity structures; several symmetric configurations that had already been found by other methods were thus re-obtained. Further applications of the same method, to slightly more complex systems will be presented next.

*Expandable octahedron*

For the expandable octahedron there are only one type of cable and strut. Knowing that the distance between parallel struts is half the length of the strut, equilibrium in the strut direction yields $q_s = -3q_c/2$. An analysis of $\mathbf{D}$ gives two possible solutions for $\mathcal{N} = 4$: $q_s = -3q_c/2$ and $q_s = -2q_c$, but $\mathbf{D}$ is positive semi-definite only for the first one. In addition to the symmetric configuration of Fig. 2, many asymmetric configurations can be found.

*Truncated tetrahedron*

An equilibrium configuration for the truncated tetrahedron was obtained in Section 2.2. For that configuration, we have computed the Singular Value Decomposition of the equilibrium matrix [35] and thus obtained the single state of self-stress of the structure. For an axial force of 1 in the cable elements forming the triangular faces, there is a force of 1.3795 in the remaining cables, and $-1.5016$ in the struts. Since the strut and cable lengths are 2.2507 and 1, respectively, the corresponding force densities are 1, 1.3795 and $-0.6672$.

We have carried out an independent form-finding study of this structure, using the force density method. Unlike all of the structures analysed so far, no general equilibrium statements can be made, since the nodes lie in four different horizontal planes, see Fig. 1. Without any relationships between the force densities, we considered a general state of self-stress characterised by three different force density values: $q_t$ for cables forming the triangles, $q_l$ for the other cables, and $q_s$ for the struts.

By setting $q_l = \gamma q_t$, and after carrying out a Gaussian elimination on the matrix $\mathbf{D}$, the

condition for $\mathcal{N} = 4$ was found to be

$$2\left(1+\gamma\right)\left(\frac{q_s}{q_t}\right)^2 + \left[3 + 2\gamma\left(3+\gamma\right)\right]\frac{q_s}{q_t} + \gamma\left(3 + 2\gamma\right) = 0 \qquad (43)$$

To re-obtain the earlier results we set $\gamma = 1.3795$ and thus re-obtained $q_s/q_t = -0.6672$, but also $q_s/q_t = -2.5022$. However, for the alternative solution $q_s/q_t = -2.5022$ the $\mathbf{D}$ matrix has negative eigenvalues, and hence the corresponding configurations are unstable.

For different values of $\gamma$, e.g. $\gamma = 1$ as in Ref. [32], different configurations of the truncated tetrahedron are obtained, with unequal cable lengths. However, if we had been interested in a particular ratio between the lengths of the cables, it would have been difficult to find the corresponding configuration with this method, as the particular values of the force densities that have to be chosen in order to achieve the required lengths cannot be determined.

Therefore, it is concluded that the force density method is an excellent method for finding the configuration of new tensegrities, but less than ideal for structures with some known, or desired element lengths.

## 5  Discussion and Conclusions

Seven form-finding methods for tensegrity structures have been reviewed and classified into two categories. The first category contains kinematical methods, which determine the configuration of either maximal length of the struts or minimal length of the cable elements, while the length of the other type of element is not allowed to vary. The second category contains statical methods, which search for equilibrium configurations that permit the existence of a state of prestress in the structure with certain required characteristics. Each category includes an analytical method, suitable only for simple or very symmetric structures.

The two remaining kinematical methods have both been used successfully to determine configuration details, i.e. the nodal coordinates, of structures that were already essentially well known. However, neither of the two can be applied to problems that are not completely defined, e.g. the lengths of all the cables are not known in the formulation where the lengths of the struts are maximised.

The three remaining statical methods are in fact only two, since the force-density method and the energy method have been shown to be equivalent. The main strength of the force density method is that it is well suited to situations where the lengths of the elements of the structure

are not specified at the start. Thus, new configurations can be easily produced, but it is difficult to control the variation in the lengths of the elements as the set of tension coefficients is varied. The reduced coordinates method offers a greater control on the shape of the structure, but involves more extensive symbolic manipulations.

# 6 Acknowledgements

# References

1. Motro, R., Foldable Tensegrities, in: S. Pellegrino, ed. *Deployable Structures*, Springer Verlag Wien-New York, 2001.

2. Skelton, R.E., *Deployable tendon-controlled structure*, United States Patent 5,642,590, July 1, 1997.

3. Caspar, D.L.D., and Klug, A., Physical principles in the construction of regular viruses, *Proceedings of Cold Spring Harbor Symposium on Quantitative Biology*, 1962, 27, 1-24.

4. Ingber, D.E., Cellular tensegrity: defining new rules of biological design that govern the cytoskeleton, *Journal of Cell Science*, 104 , 1993, 613-627.

5. Marks, R. and Fuller, R.B., *The Dymaxion World of Buckminster Fuller*, Reinhold Publications, New York, 1960.

6. Fuller, R.B., *Tensile-integrity structures*, United States Patent 3,063,521, November 13, 1962.

7. Snelson, K.D., *Continuous tension, discontinuous compression structures*, United States Patent 3,169,611, February 16, 1965.

8. Pugh, A., *An Introduction to Tensegrity*, University of California Press, Berkeley, California, 1976.

9. Motro, R., Tensegrity systems: the state of the art, *International Journal of Space Structures*, 7 (2), 1992, 75-83.

10. Connelly, R. and Terrell, M., Globally rigid symmetric tensegrities, *Structural Topology*, 21 , 1995, 59-78.

11. Vassart, N. and Motro, R., Multiparametered formfinding method: application to tensegrity systems, *International Journal of Space Structures*, 14 (2), 1999, 147-154.

12. Sultan, C., Corless, M., and Skelton, R.E., Reduced prestressability conditions for tensegrity structuresed., *Proceedings of 40th AIAA/ASME/ASCE/AHS/ASC Structures, Structural Dynamics and Materials Conference*, 12-15 April 1999, St Louis, MO, AIAA, 1999.

13. Pellegrino, S., *Mechanics of kinematically indeterminate structures*, Ph.D. dissertation, University of Cambridge, U.K., 1986.

14. MathWorks, *Matlab User's Guide, version 5*, 1997.

15. Day, A. and Bunce, J., The analysis of hanging roofs, *Arup Journal*, September , 1969, 30-31.

16. Barnes, M.R., Form-finding and analysis of prestressed nets and membranes, *Computers & Structures*, 30 (3), 1988, 685-695.

17. Motro, R., Forms and forces in tensegrity systems, in: H. Nooshin, ed., *Proceedings of Third International Conference on Space Structures*, Elsevier, Amsterdam, 1984, 180-185.

18. Belkacem, S., *Recherche de forme par relaxation dynamique des structures reticulees spatiales autoconstraints*, Ph.D. Dissertation, L'Universite Paul Sabatier de Toulouse, 1987.

19. Motro, R., Tensegrity systems and geodesic domes, *International Journal of Space Structures*, 5 (3-4), 1990, 341-351.

20. Motro, R., Belkacem, S., and Vassart, N., Form finding numerical methods for tensegrity systems, in: J.F. Abel, J.W. Leonard, and C.U. Penalba, ed., *Proceedings of IASS-ASCE International Symposium on Spatial, Lattice and Tension Structures*, Atlanta, USA, ASCE, 1994, 707-713.

21. Kenner, H., *Geodesic Math and How to Use It*, University of California Press, Berkeley, California, 1976.

22.  Schek, H.-J., The force density method for form finding and computation of general networks, *Computer Methods in Applied Mechanics and Engineering*, 3, 1974, 115-134.

23. Linkwitz, K., Formfinding by the "direct approach" and pertinent strategies for the conceptual design of prestressed and hanging structures, *International Journal of Space Structures*, 14 (2), 1999, 73-87.

24.  Southwell, R.V., *An Introduction to the Theory of Elasticity*, Dover Publications, New York, 1969.

25.  Barnes, M.R., Applications of dynamic relaxation to the design of cable, membrane and pneumatic structures., in: W.J. Supple, ed., *Proceedings of Second International Conference on Space Structures*, Guildford, 1975.

26.  Lai, C.Y., You, Z., and Pellegrino, S., Shape of deployable membrane reflectors, *ASCE Journal of Aerospace Engineering*, 11 (July), 1998, 73-80.

27.  Vassart, N., *Recherche de forme et stabilité des systèmes réticulés spatiaux autocontraints: Applications aux systèmes de tenségrité*, Ph.D. Dissertation, Université des Sciences et Techniques du Languedoc, Montpellier, France, 1997.

28.  Connelly, R., Rigidity, in: P.M. Gruber and J.M. Wills, ed., *Handbook of Convex Geometry*, Elsevier Publishers Ltd, 1993, 223-271.

29.  Connelly, R., Rigidity and energy, *Inventiones Mathematicae*, 66 (1), 1982, 11-33.

30.  Kötter, E., Über die Möglichkeit, $n$ Punkte in der Ebene oder im Raume durch weniger als $2n - 3$ oder $3n - 6$ Stäbe von ganz unveränderlicher Länge unverschieblich miteinander zu verbinden, in: *Festschrift Heinrich Müller-Breslau*, A. Kröner, Leipzig, 1912, 61-80.

31.  Connelly, R., Tensegrity structures: why are they stable?, in: M.F. Thorpe and P.M. Duxbury, ed., *Rigidity theory and applications*, Plenum Press, New York, 1999, p. 47-54.

32.  Connelly, R. and Back, A., Mathematics and tensegrity, *American Scientist*, 86 (2), 1998, 142-151.

33.  Sultan, C., *Modeling, design, and control of tensegrity structures with applications*, Ph.D. Dissertation, Purdue University, 1999.

34.  Strang, G., *Linear Algebra and its Applications*, Third edition, Harcourt Brace Jovanovich

College, San Diego, 1988.

35.  Pellegrino, S., Structural computations with the Singular Value Decomposition of the equilibrium matrix, *International Journal of Solids and Structures*, 30 (21), 1993, 3025-3035.

Table 1: Values of $\theta$ for symmetric tensegrity prisms.

| $v$ | $j$ | | | | |
|---|---|---|---|---|---|
| | 1 | 2 | 3 | 4 | 5 |
| 3 | 30° | −30° | — | — | — |
| 4 | 45° | 0° | −45° | — | — |
| 5 | 54° | 18° | −18° | −54° | — |
| 6 | 60° | 30° | 0° | −30° | −60° |

(a) Side view          (b) Top view
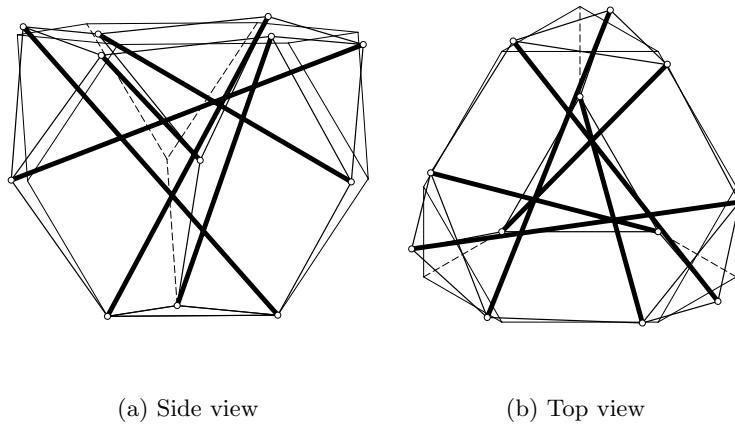
Figure 1: Comparison of truncated tensegrity tetrahedron and the polyhedron from which it originates. Note the distortion of the hexagonal faces. Hidden lines of the polyhedron shown dashed.



(a) Side view          (b) Top view
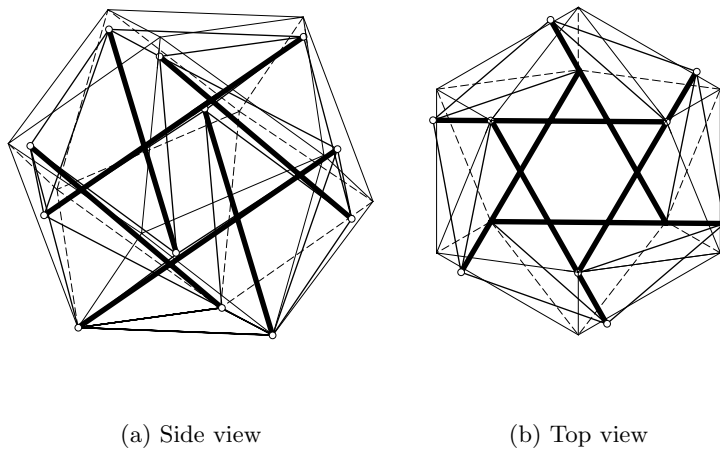
Figure 2: Comparison of expandable octahedron and icosahedron. Hidden lines of the polyhedron shown dashed.
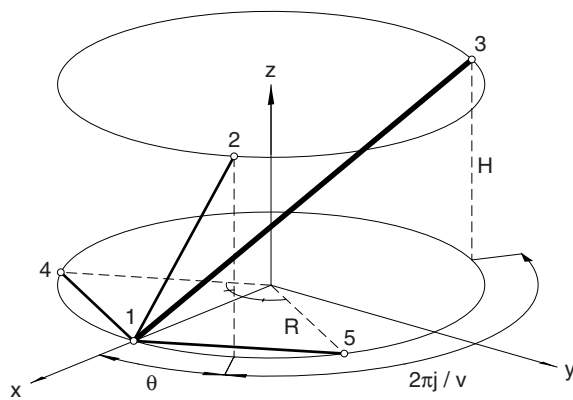


Figure 3: Elements meeting at node 1 of structure with $v$-fold symmetry, with radius $R$ and height $H$.
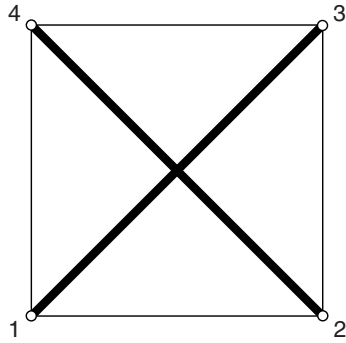
Figure 4: Snelson's X-frame



(a) (b)
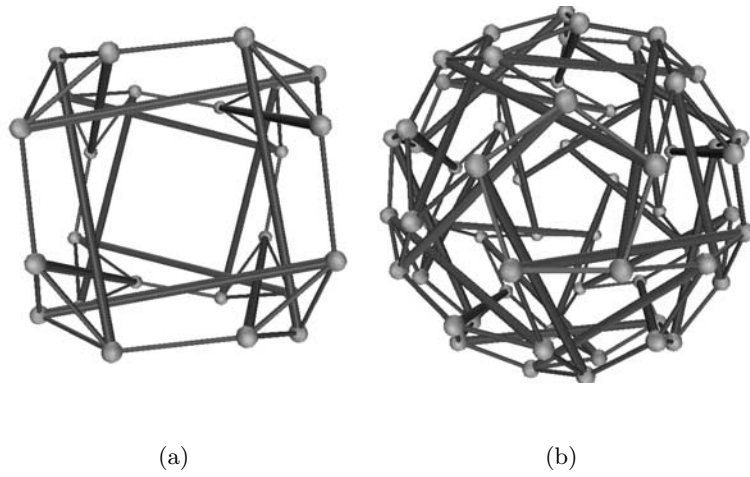
Figure 5: Symmetric tensegrities from Connelly and Back's catalogue, see Ref. [32].
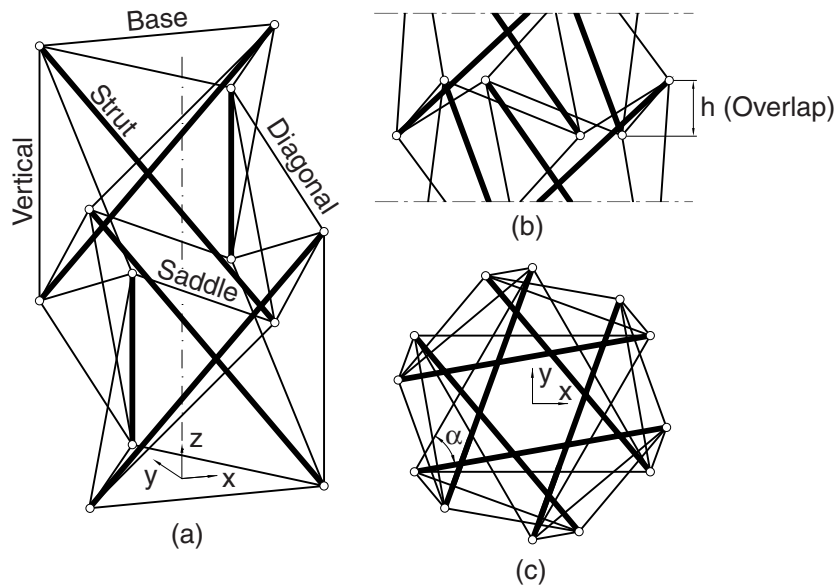


Figure 6: Two stage tensegrity tower: (a) perspective view, (b) side view of central part, and (c) top view.
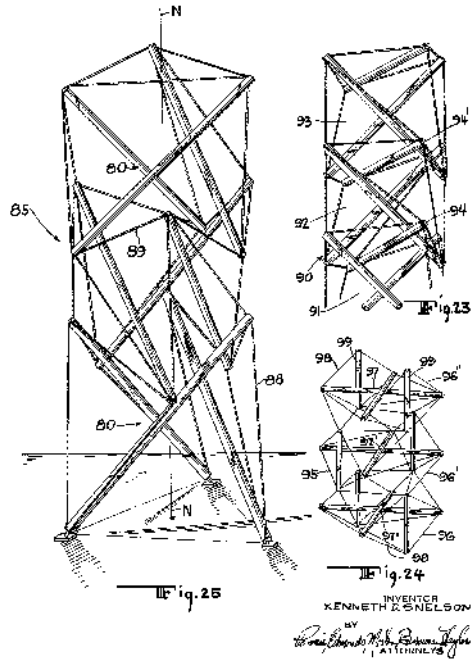
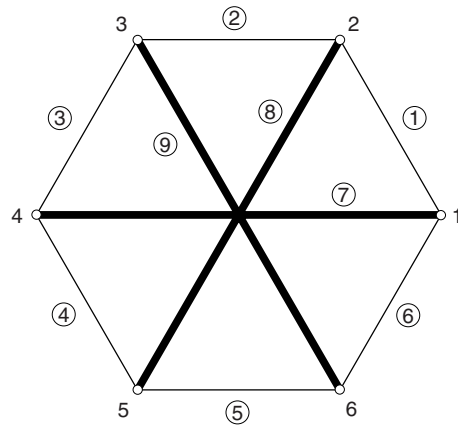Figure 7: Three stage tensegrity tower, reproduced from Ref.[ 7].



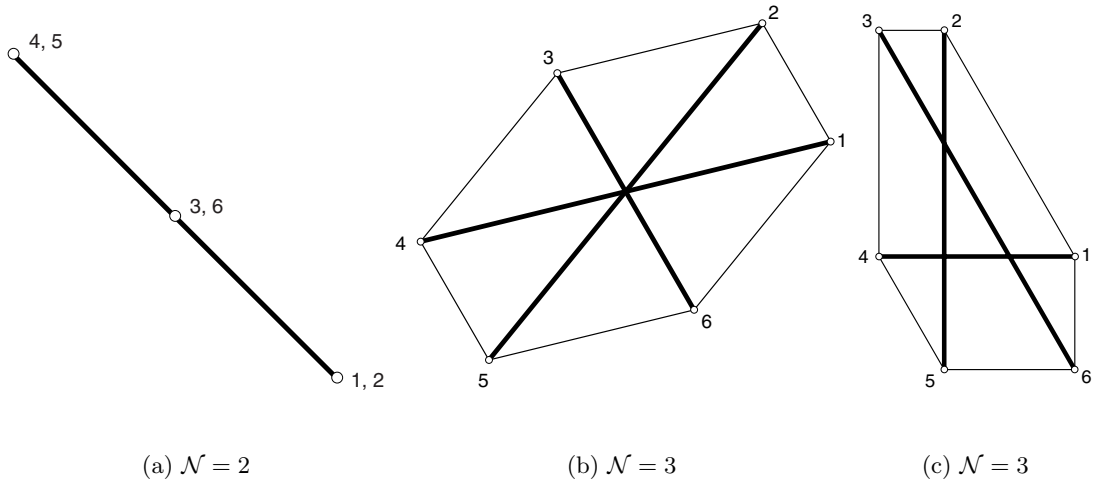Figure 8: Two-dimensional hexagonal tensegrity.

(a) $\mathcal{N} = 2$                    (b) $\mathcal{N} = 3$                    (c) $\mathcal{N} = 3$

Figure 9: Configurations of two-dimensional hexagonal tensegrities.



Figure 10: Tensegrity prism.



(a) $q_t = q_b$, $q_l = \sqrt{3}q_b$, and         (b) $q_t = q_l$, $q_b = q_l/3$, and

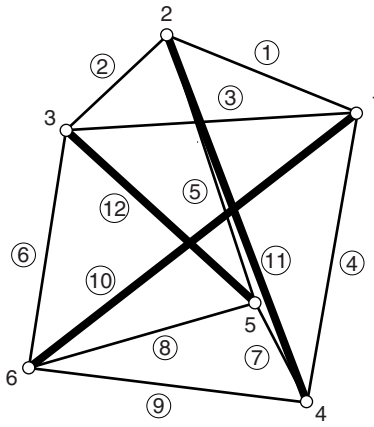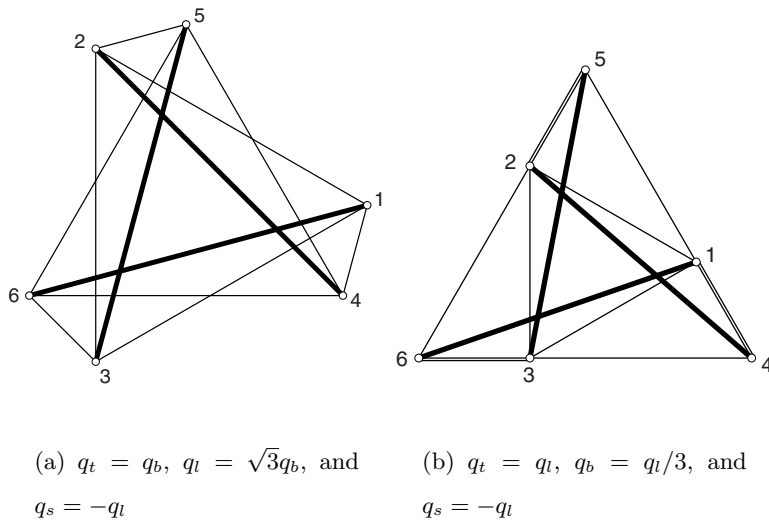$q_s = -q_l$                              $q_s = -q_l$

Figure 11: Top views of two different rotationally symmetric tensegrity prism.